High Frequency Flow Measurement Technique for Slug Flow Regimes

Seyyed Saeed Shojaee Zadeh[1,2], Vanessa Egan[1,2], Pat Walsh[2]
[1] CONNECT, Stokes Laboratories, Bernal Institute, University of Limerick, Ireland, V94T9PX
[2] School of Engineering, University of Limerick, Ireland, V94T9PX
Saeed.zadeh@ul.ie, Vanessa.egan@ul.ie, Pat.walsh@ul.ie

Abstract *– To achieve accurate slug lengths and velocities in slug flow regime, monitoring of the droplet/bubble train is an essential stage which necessitates the use of proper techniques. In most experiments, the traditional measurement apparatus consists of a high-speed camera coupled to a microscope which are employed to characterize such flows in microchannels. However, when using these techniques, optical distortion caused by the curved channel walls can result in large measurement uncertainty which undermines the measurement accuracy. In this regard, this study introduces a novel technique to easily and reliably measure the slug length and velocity. This automated non-intrusive measurement technique allows in-line high-frequency of droplet/bubble detection and related physical properties based on changes in the light intensity caused by a phase shifting in liquid-liquid or liquid-gas flows.*

Keywords: slug flows, non-intrusive technique, in-line, high-frequency

1. Introduction

Slug flow, also commonly known as Taylor flow, consists of two immiscible fluids moving within a channel. One of the fluids, the carrier phase, wets the channel wall and entirely engulfs the second fluid known as the dispersed/droplet phase. The second phase is present as discrete slugs/droplets within the carrier phase. In microchannels, slug flows have the advantage of high surface -to-volume ratios and internal circulations which not only promote thermal transfer from the channel wall but also mass transfer between phases[1-3]. Numerous experimental and numerical studies have demonstrated higher heat transfer rates of up to 700% when compared to standard single phase flows[4]. Slug flows are also used in microreactors, microfiltration, and catalytic processes to increase mixing rates and efficiency[5-7].

To attain the best performance in applications that benefit from slug flows, designers must have a thorough understanding of the flow configuration. Due to the small physical dimensions of such microfabricated devices, non-intrusive measurement techniques with high resolution are required to assess flow properties. In recent decades, microchannel flows are studied using a range of imaging techniques. The most common method is optical microscopy, which involves illuminating the flow from underneath with a powerful light source and inspecting it from above with a short camera shutter length. This method typically needs complicated and expensive instrumentation, such as microscopes with integrated high-speed cameras and a powerful light source, restricting adaptability and providing only narrow-time assessments[8]. Furthermore, the accuracy of the data obtained is heavily reliant on the camera's resolution and the operator's skill. Optical distortion caused by curved channel walls or varying refractive index may also cause significant measurement inaccuracy. Particularly, in circular microchannels with extremely small radii, optical distortion is a major issue for flow imaging. In addition, this technique does not allow in-line assessment and to obtain results, post processing of images is necessary. Therefore, researchers have found it challenging to develop precise and suitable apparatus for in-line assessment of flow characteristics in microscale two-phase flows.

In this regard, the current study proposes a novel measurement technique for investigating flow properties in both liquid-liquid and liquid-gas slug flow regimes. Regardless of channel shape, this non-intrusive approach allows in-line measurements of both carrier and dispersed phase length and velocity with excellent precision. This measurement methodology will aid in the determination and analysis of two-phase flow configurations in transparent microchannels, allowing for a better comprehension of the experimental data.

2. Measurement Technique

The automation of droplet recognition and related physical features such as droplet length and velocity are based on the difference in light transmission through a tube caused by phase shifting in liquid-liquid or liquid-gas flows. In this regard, a reliable light source that delivers a steady amount of light orthogonal to the length-axis of the tubing, as well as a sensor sensitive to light intensity, are required to identify the fluctuation in transmitted light caused by phase shifting. In the current investigation, standard white LEDs with a maximum Voltage of 3.4V and a maximum current of 50mA were employed as a light source and Burr-Brown photodiodes with an integrated amplifier, model OPT301M,

were utilized to detect the transmitted light. To keep system noise to a minimal level, the electrical hosing was grounded by a differential ground and shielded cables were used.

To accurately locate the LED and photodiode at a specific axial location along the tube and orthogonal to the tube axis, a holder was designed and 3D printed from PLA (see Fig. 1(a)). The holder also shielded the photodiode from outside light.
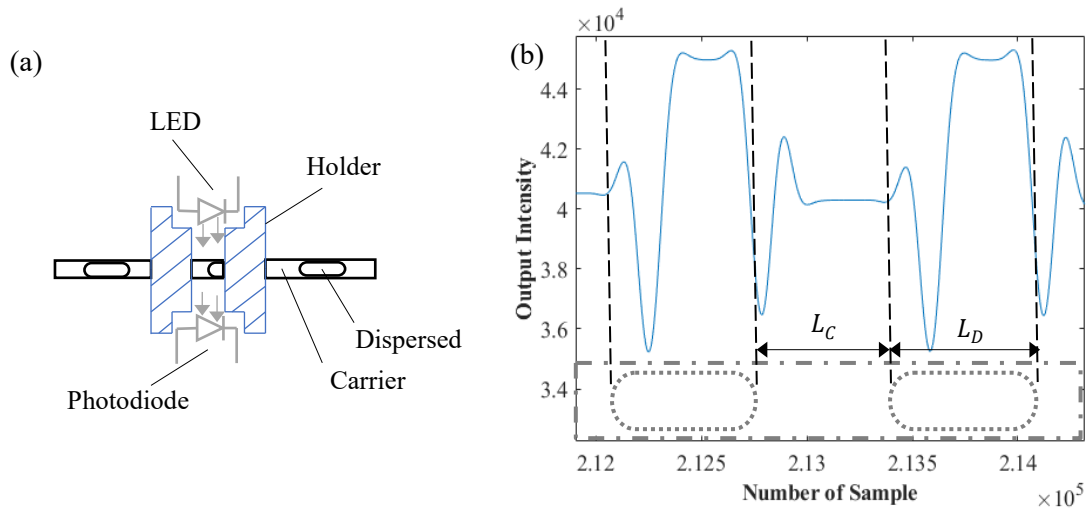
Fig. 1: **(a)** Configuration of the light sensor; **(b)** an example of recorded data for droplet velocity and length measurements.

The variation in light intensity recorded by the photodiode can be attributed to two factors. The first is due to a different light transmission coefficient between fluids. In liquid-liquid flows, due to the comparable refractive indices of the liquids, the change in light transmission is expected to be minimal. The second and more important effect is the dispersion caused by light refraction and reflection at the interface between the dispersed and carrier liquids. Although this technique can be used in both liquid-liquid and liquid-gas flows, the current study focuses on liquid-liquid flows to analyse the worst-case scenario in which there is a small difference in refractive index between the liquids. Water and AR20 with refractive indices of 1.33 and 1.44 were utilized within a circular capillary with an inner diameter of 0.8mm. In order to generate slug trains, both liquids were drawn into the tube by simultaneously vertically plunging a traverse, which held one end of the tube, into a reservoir containing both immiscible fluids while using a syringe pump situated at other end of the tube in withdraw mode. A G-Code program was used to regulate and sync the traverse system and the syringe pump to generate droplet trains with different dispersed and carrier phase lengths. An example of an output signal from the photodiode is shown in figure 1(b). In this case, water and AR20 are the dispersed and continuous phases respectively with results shown for two droplets.

To better comprehend the signal post-processing and how the droplet length was determined, Figure 2 displays a sample of the output signal from an individual droplet as well as a schematic graph demonstrating the reflection effects. The analogy to a sideward exposed hemispherical lens, which bundles or scatters light depending on the position of the light beam, explains why the cap surfaces have such a strong influence. Several images were taken using a high-speed camera from droplets of various lengths to confirm the correctness of the signal processing.

(I) The droplet front cap has yet to be introduced, the light is perfectly aligned, and the signal intensity remains constant.

(II) Light reflection towards the photodiode, caused by the front cap, can explain the partial rise in light intensity. This light cannot travel through the light channel towards the photodiode in an undisturbed situation.

(III) As the droplet advances, the front cap reflects a significant quantity of light that would otherwise be transmitted to the photodiode. Additionally, due to the lower refractive index of water and cap curvature, a portion of the aligned-light is deflected towards the outside of the sensor window.

(IV) Beyond the caps, when the center of the droplet is aligned with the LED and sensor, there is a difference in the voltage output compared to the carrier fluid. The difference is due to the fluid's transparency, with water being more transparent than AR20.

(V) Light scattering caused by the rear cap results in a lesser amount of incoming light to the photodiode.

(VI) Similar to II, reflection effect of the rear cap on non-aligned light can explain the rise in light intensity.

(VII) Similar to (I), the droplet has passed the light window.

It is also worth noting that different fluid combinations, as well as changes in the holder, tubing diameter, and light intensity, result in slightly different recorded signals.
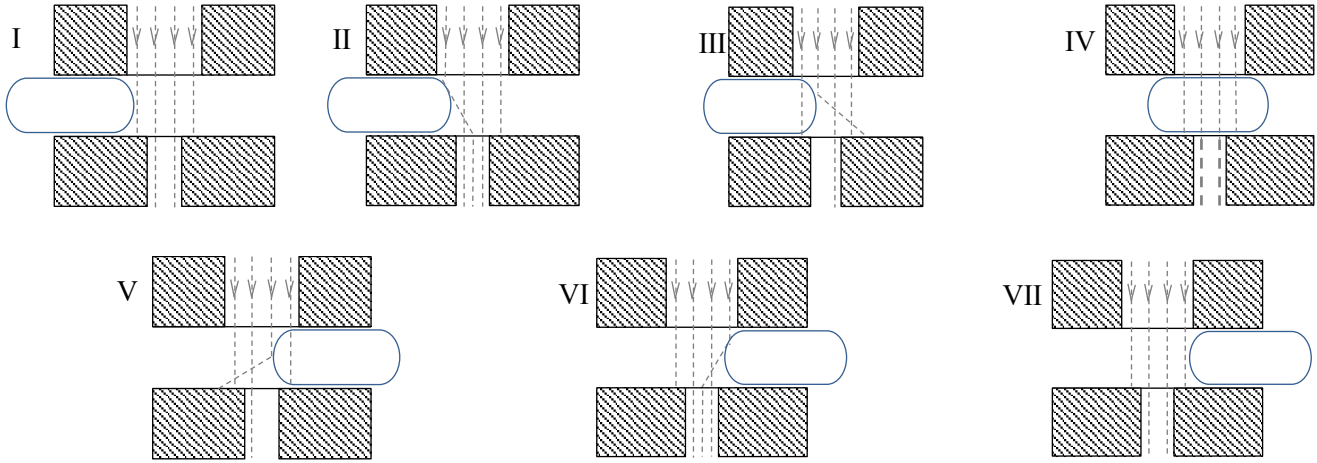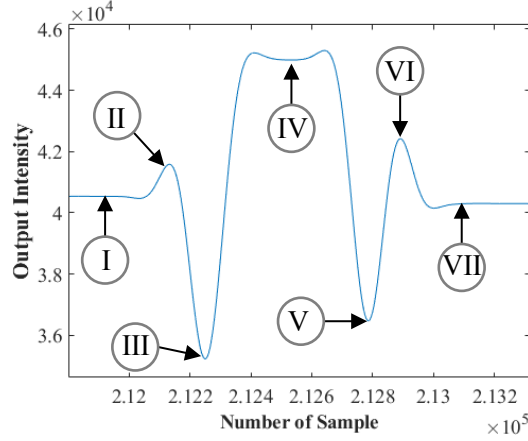
Fig 2: Signal intensity variations due to the light reflection and deflection effects caused by droplet caps. In this case, water droplet is dispersed in AR20.

Once the front and rear caps of the droplets have been detected, the velocity of each droplet can be simply determined by measuring the elapsed time it takes for the droplet to travel from one sensor to the next when placed at a specific distance (l) apart. The elapsed time (t) is determined based on the sample frequency (f) and amount of recorded samples (n). In this study, two photodiodes were set at one meter apart and data was recorded at a frequency of 10kHz. The length of a droplet (L_D) can be calculated using the droplet velocity (U_D) and the time it takes for the droplet to pass a single sensor. As a result, the length of the continuous phase (L_C) can be determined by knowing the times assigned to the back cap of one droplet and the front cap of the following droplet.

$$t = \frac{n}{f} \tag{1}$$

$$U_D = \frac{l}{t} \tag{2}$$

$$L_{D_i} = U_{D_i} \times t_{r_i} - t_{f_i} \tag{3}$$

$$L_{C_i} = U_{D_i} \times (t_{f_{i+1}} - t_{r_i}) \tag{4}$$

t_r and t_f are the times assigned to rear and front caps respectively.

A data acquisition unit was set up to collect the data from two photodiodes and a custom MATLAB code was written for post processing of the output signal. This system setup allows for an in-line evaluation over the flow

characteristics, as well as the storage of data on an SD memory card for subsequent analysis. Figure 3 presents results for carrier and dispersed (droplet) phase measurement obtained from a trial with 120 water droplets.
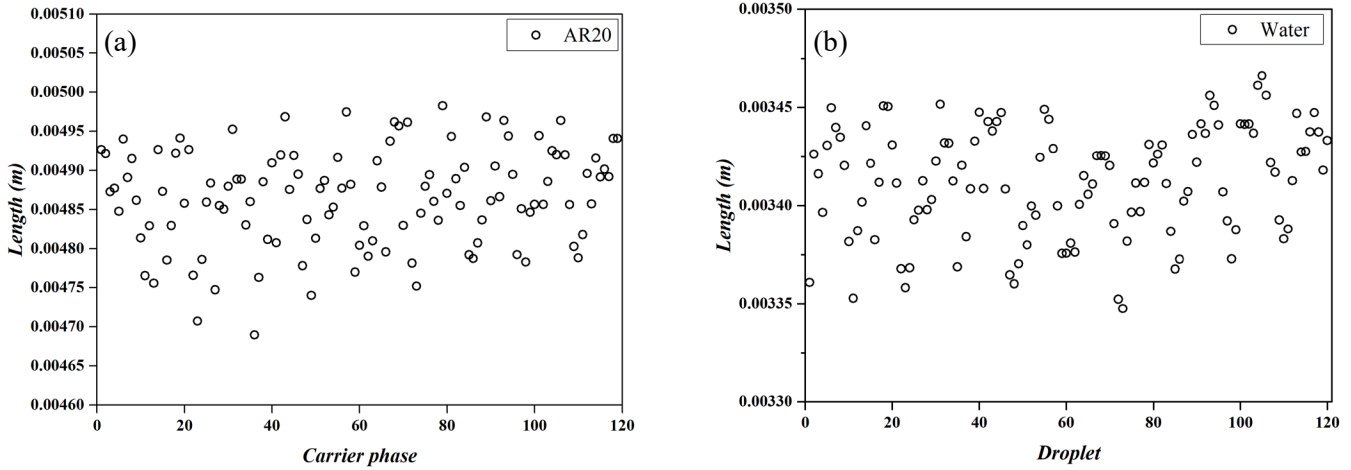
Fig. 3: Sample data from measurements of (a) carrier length and (b) dispersed phase (droplet) length. In this example, 120 droplets of water are dispersed within AR20.

This measurement technique may also be used to determine the inner diameter of the tubing by filling a certain length of the tube at a certain flow rate (Q) and measuring the time (Δt) it takes for the phase to shift from air to liquid. Two photodiode sensors, one meter apart, were used in this work to determine the exact phase changing time. The diameter can be calculated by following equation:

$$D = 2\sqrt{\frac{Q\Delta t}{\pi l}} \tag{5}$$

The actual diameter was measured to be 6% less than nominal diameter given by the manufacturer. It is important in this procedure to use the tube that has not been used before because any trace of liquid within the tube causes the diameter to be measured lower than the actual value.

3. Conclusion

This study presents a novel measurement technique to determine droplet and carrier length and velocity for slug flows within macro and micro transparent channels. This non-intrusive method provides an in-line high-frequency platform for measuring flow characteristics of liquid-liquid and liquid-gas flows in channels of any cross-sectional geometric shape. This methodology also enables a reliable framework to determine the inner diameter of tubing with a high precision.

Acknowledgements

References

[1] A. Abdollahi, S. E. Norris, and R. N. Sharma, "Fluid flow and heat transfer of liquid-liquid Taylor flow in square microchannels," *Applied Thermal Engineering,* vol. 172, p. 115123, 2020.
[2] M. N. Kashid, A. Gupta, A. Renken, and L. Kiwi-Minsker, "Numbering-up and mass transfer studies of liquid–liquid two-phase microstructured reactors," *Chemical Engineering Journal,* vol. 158, no. 2, pp. 233-240, 2010.
[3] M. T. Kreutzer, F. Kapteijn, J. A. Moulijn, and J. J. Heiszwolf, "Multiphase monolith reactors: chemical reaction engineering of segmented flow in microchannels," *Chemical Engineering Science,* vol. 60, no. 22, pp. 5895-5916, 2005.
[4] M. M. G. Eain, V. Egan, and J. Punch, "Local Nusselt number enhancements in liquid–liquid Taylor flows," *International Journal of Heat and Mass Transfer,* vol. 80, pp. 85-97, 2015.

[5] J. Burns and C. Ramshaw, "The intensification of rapid reactions in multiphase systems using slug flow in capillaries," *Lab on a Chip,* vol. 1, no. 1, pp. 10-15, 2001.

[6] A. Cybulski and J. A. Moulijn, *Structured catalysts and reactors*. CRC press, 2005.

[7] G. Qian, J. Zhou, J. Zhang, C. Chen, R. Jin, and W. Liu, "Microfiltration performance with two-phase flow," *Separation and purification technology,* vol. 98, pp. 165-173, 2012.

[8] M. Robert de Saint Vincent, S. Cassagnère, J. Plantard, and J.-P. Delville, "Real-time droplet caliper for digital microfluidics," *Microfluidics and nanofluidics,* vol. 13, no. 2, pp. 261-271, 2012.